

Functions of the Bloom Syndrome Helicase N-terminal Intrinsically Disordered Region

Colleen C. Bereda*¹, Evan B. Dewey*^{2,3}, Mohamed A. Nasr⁴, and Jeff Sekelsky^{1,2,3,4}

¹ Department of Biology

University of North Carolina at Chapel Hill

Chapel Hill, NC 27599

² Lineberger Comprehensive Cancer Center

University of North Carolina at Chapel Hill

Chapel Hill, NC 27599

³ Integrative Program for Biological and Genome Sciences

University of North Carolina at Chapel Hill

Chapel Hill, NC 27599

⁴ Curriculum in Genetics and Molecular Biology

University of North Carolina at Chapel Hill

Chapel Hill, NC 27599

* Correspondence: sekelsky@unc.edu

Running title: Functions of Blm helicase N-terminal IDR

1 Abstract

2 Bloom Syndrome helicase (Blm) is a RecQ family helicase involved in DNA repair, cell-cycle
3 progression, and development. Pathogenic variants in human *BLM* cause the autosomal
4 recessive disorder Bloom Syndrome, characterized by predisposition to numerous types of
5 cancer. Prior studies of *Drosophila Blm* mutants lacking helicase activity or protein have shown
6 sensitivity to DNA damaging agents, defects in repairing DNA double-strand breaks (DSBs),
7 female sterility, and improper segregation of chromosomes in meiosis. Blm orthologs have a
8 well conserved and highly structured RecQ helicase domain, but more than half of the protein,
9 particularly in the N-terminus, is predicted to be unstructured. Because this region is poorly
10 conserved across multicellular organisms, we compared closely related species to identify
11 regions of conservation, potentially indicating important functions. We deleted two of these
12 *Drosophila*-conserved regions in *D. melanogaster* using CRISPR/Cas9 gene editing and
13 assessed the effects on different Blm functions. Each deletion had distinct effects on different
14 Blm activities. Deletion of either conserved region 1 (CR1) or conserved region 2 (CR2)
15 compromised DSB repair through synthesis-dependent strand annealing and resulted in
16 increased mitotic crossovers. In contrast, CR2 is critical for embryonic development but CR1 is
17 not as important. CR1 deletion allows for proficient meiotic chromosome segregation but does
18 lead to defects in meiotic crossover designation and patterning. Finally, deletion of CR2 does
19 not lead to significant meiotic defects, indicating that while each region has overlapping
20 functions, there are discreet roles facilitated by each. These results provide novel insights into
21 functions of the N-terminal disordered region of Blm.

22 Introduction

23 Bloom syndrome helicase (Blm in *Drosophila*; BLM in humans) is an ATP-dependent,
24 RecQ family helicase (5-7). It is conserved across protists, plants, fungi, and animals, with roles
25 in homology-directed DNA repair (HDR), cell-cycle progression, meiosis, and development (1, 3,
26 8-16). Pathogenic variants in *BLM* cause Bloom Syndrome, a rare autosomal recessive disorder
27 characterized by a high predisposition to a broad range of cancers, sun sensitivity, short-stature,
28 sterility, and immunodeficiency (5, 17, 18). *BLM* mutations have also been found in sporadic
29 cancers (19-22). The high predisposition to cancer in individuals with Bloom Syndrome is
30 associated with genome instability, including high rates of exchange between sister chromatids
31 and homologous chromosomes (23, 24).

32 One important function of BLM/Blm in HDR is disassembly of DNA repair intermediates,
33 which is done in concert with topoisomerase III alpha (*TopIII α*) (25-28). BLM and *TopIII α* ,
34 together with RMI1 (which *Drosophila* lacks (29)), unwind D-loops to promote dissociation of the
35 invading strand in synthesis-dependent strand annealing (SDSA) (2, 7, 25, 27) and catalyzes
36 dissolution of double Holliday junctions (dHJs) (13, 26, 30-32). These two functions prevent
37 mitotic crossovers and therefore minimize loss of heterozygosity (LOH) and chromosome
38 rearrangement. Blm orthologs also have functions in meiosis, but these include promoting
39 crossovers (reviewed in 14). In *Drosophila*, loss of Blm results in decreased meiotic crossover
40 rates, compromised crossover distribution and increased chromosome mis-segregation (non-
41 disjunction) (1).

42 BLM/Blm also has functions in repair of stalled replication forks to promote an efficient S-
43 phase (12, 25). BLM accumulates at stalled forks along with other DNA repair regulators, with *in*
44 *vitro* studies suggesting BLM may act to regress stalled forks behind a DNA lesion to promote
45 lesion removal by other repair pathways (33, 34). A second BLM cell cycle role is to resolve
46 anaphase bridges to allow proper chromosome segregation during mitosis (35, 36). In human

47 cells, this activity is mediated through interaction with topoisomerase II α (TopII α) (37).
48 Micronuclei and aneuploidy are more prevalent in *BLM*-deficient cells, underscoring the
49 importance of this BLM role to genome stability (38, 39). In *Drosophila*, embryos lacking Blm
50 have increased anaphase bridges during rapid syncytial cell cycles, resulting in high rates of
51 embryonic death (3, 16). These various functions suggest that BLM/Blm regulation is dependent
52 on cell type and developmental timing.

53 While BLM/Blm is best known by its RecQ helicase domain, there are large, intrinsically
54 disordered regions (IDRs) both N- and C-terminal to this domain (Figure 1A). These regions,
55 though poorly conserved in primary sequence, are likely candidates for both regulatory
56 modifications and protein-protein interactions. TopIII α is thought to bind in at least one of these
57 regions, and other proteins' interactions have been mapped to them as well (28, 37, 40).
58 Despite this, the IDRs have been relatively poorly explored compared to the helicase domain,
59 even though they make up more than half of the protein (Figure 1A). A study in *Drosophila*
60 underscores the importance of these regions, with a *Blm* allele that deletes most of the
61 unstructured N-terminus (*Blm*^{N2}) compromising HDR and meiotic roles while only mildly affecting
62 early embryonic functions (Figure 1B) (3).

63 To further investigate the function of the intrinsically disordered N-terminal region, we
64 characterized the impacts of deletions of two N-terminal regions conserved in closely related
65 *Drosophila* species on embryonic development, HDR, and meiosis. We find that while deletion
66 of the first 240 amino acids does not compromise Blm in meiotic chromosome segregation, it
67 does affect embryonic development, HDR, and meiotic crossover distribution, albeit less
68 severely than *Blm* null mutations. A deletion of the 146 amino acids just prior to the start of the
69 structured RecQ helicase domain results in severe defects in cell division and development but
70 has milder effects on HDR and apparently normal meiotic crossover distribution and

71 segregation. These findings highlight the importance of investigating intrinsically disordered Blm
 72 regions to understanding function.

73

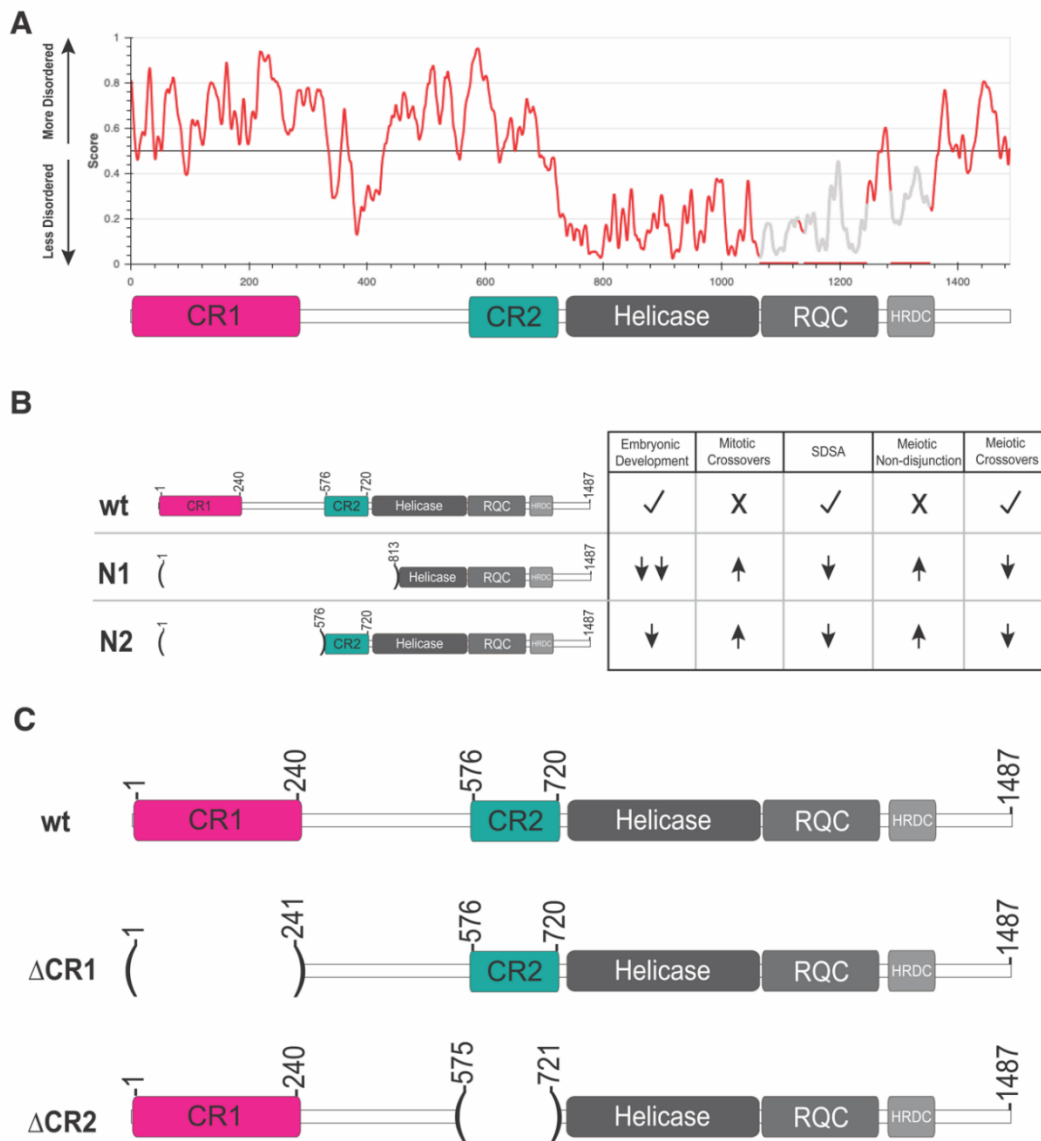


Figure 1. Bloom syndrome helicase (Blm) predicted structural order and alleles used. (A) IUPred3 (2) plot predicting the ordered and intrinsically disordered regions of Blm. A schematic of Blm domains is placed below for reference, illustrating that conserved regions 1 and 2 (CR1 and CR2) are predicted to be mostly disordered (>0.5). **(B)** Previously characterized alleles of *Blm* and their effects on Blm functions relative to wild-type (wt). A null allele, *Blm*^{N1} (N1) eliminates all well-characterized Blm functions, while the separation-of-function allele *Blm*^{N2} (N2) only moderately affects embryonic development. **(C)** Schematic of Blm deletions used compared to the wt Blm protein. Δ CR1 deletes amino acids 2-240, preserving amino acids 241-1487 in frame; Δ CR2 deletes amino acids 576-720, fusing amino acids 1-575 and 721-1487 together in frame.

74 Results

75 Identification of N-terminal regions conserved among *Drosophila* species and deletion by 76 CRISPR/Cas9 genome editing

77 Despite high conservation in the helicase domain of Blm, the roughly 720 amino acid N-
78 terminal region is not well conserved among multicellular organisms. This region is predicted to
79 be intrinsically disordered (Figure 1A). Prior studies the *Blm*^{N2} allele, which deletes the first 575
80 residues of the IDR but retains 146 residues upstream of the helicase domain pointed to a
81 potential role of this helicase-adjacent N-terminal region in embryonic development (McVey,
82 2007). To further examine functions of the N-terminal region, we narrowed our focus to
83 conservation among more closely related *Drosophila* species (Figure S1). Alignment of these
84 species identified two regions of high similarity, which we term conserved region one (Figure
85 1C, CR1; amino acids 1-240) and conserved region two (Figure 1C; CR2; amino acids 533-
86 720). CR1 may contain one of the two regions in human BLM found to interact with TopIII α (28).
87 We further narrowed CR2 to contain only the N-terminal amino acids predicted to present in the
88 protein produced by the *Blm*^{N2} allele (amino acids 576-720), to compare their functions more
89 directly. Using CRISPR/Cas9 genome editing, we separately deleted the sequences encoding
90 amino acids 1-240 and 576-720 in the endogenous *Blm* gene (Figure S2). We refer to these
91 alleles as *Blm* ^{Δ CR1} and *Blm* ^{Δ CR2}.

92

93 Embryonic hatch rates are affected differently by each N-terminal Blm deletion

94 The absence of maternally supplied Blm results in frequent anaphase bridges and high
95 rates of embryonic lethality (3, 16). To determine the effects of each deletion on Blm function in
96 embryonic development, we conducted embryonic hatching assays. In agreement with prior
97 results, embryos from females homozygous for the *Blm*^{N1} allele, which does not produce Blm
98 transcript or protein (3), have severely reduced hatch rates. In contrast, there is much smaller,

99 though significant, reduction in hatching of embryos from *Blm*^{N2} mothers (Figure 2).
100 Functionality of the *Blm*^{N2} protein in embryogenesis likely requires the presence of the helicase,
101 RecQ, and HRDC domains, but the predicted *Blm*^{N2} protein also has the last 146 residues of the
102 N-terminal IDR that may contribute to function. We assessed the effects of deletion of this
103 region (CR2) on embryogenesis (Figure 2). Strikingly, embryos from *Blm*^{ΔCR2} females have a low
104 hatch rate similar to that of embryos from *Blm*^{N1} mothers, consistent with this region being
105 critical to Blm function in embryonic development.

106 We also assayed the effects of the CR1 deletion on hatching. While the fraction of
107 embryos from *Blm*^{ΔCR1} females that hatched was significantly lower than that of embryos from wild-
108 type females, it was significantly higher than that of embryos from either *Blm*^{ΔCR2} or *Blm*^{N1}
109 females (Figure 2), indicating that this region is less important to Blm roles in embryonic
110 development. This was consistent with the high hatch rate of embryos from *Blm*^{N2} mothers,
111 which also significantly lower than that of wild-type but higher than that of *Blm*^{ΔCR2} and *Blm*^{N1}, in
112 line with previous findings (CITE McVey 2007).

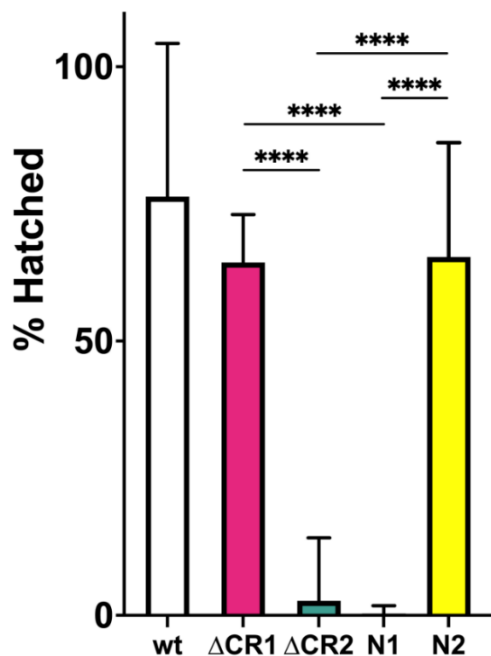


Figure 2. Hatching of embryos from *Blm* mutant mothers. Virgin females homozygous for the *Blm* alleles indicated on the X-axis were crossed to Oregon-RM males and allowed to lay overnight on grape-juice agar. Embryos were transferred to fresh grape-juice agar plates and scored for hatching 48 hours later. Each experiment was repeated three times, with 100-250 embryos transferred each time. Embryos from *Blm*^{ΔCR2} (ΔCR2) or *Blm*^{N1} (N1) females are rarely able to complete development. Embryos from *Blm*^{ΔCR1} (ΔCR1) and *Blm*^{N2} (N2) have a modest but significant reduction in hatch rates. We conclude that the CR2 region is more critical for embryonic development but the CR1 region contributes only to a small degree. *n* = wt: 598; ΔCR1: 1080; ΔCR2: 743; N1: 706; N2: 700. **** *p* < 0.0001 by Fisher's exact test.

113 **Mitotic crossovers are moderately elevated in *Blm*^{ΔCR1} and *Blm*^{ΔCR2} mutants**

114 Flies with the *Blm*^{N1} or *Blm*^{N2} deletion have elevated spontaneous mitotic crossovers,
115 probably due at least in part to compromised SDSA and/or dHJ dissolution functions (Figure 1B)
116 (3, 11). We assayed *Blm*^{ΔCR1} and *Blm*^{ΔCR2} mutants and found they also have elevated mitotic
117 crossovers (Figure 3), but at rates (0.28% and 0.61%, respectively) that are significantly lower
118 than those of *Blm*^{N1} and *Blm*^{N2} alleles (2.3% and 2.4%, respectively). This suggests that loss of
119 CR1 or CR2 allows some non-crossover repair or some other function that prevents lesions that
120 can be repaired as crossovers.

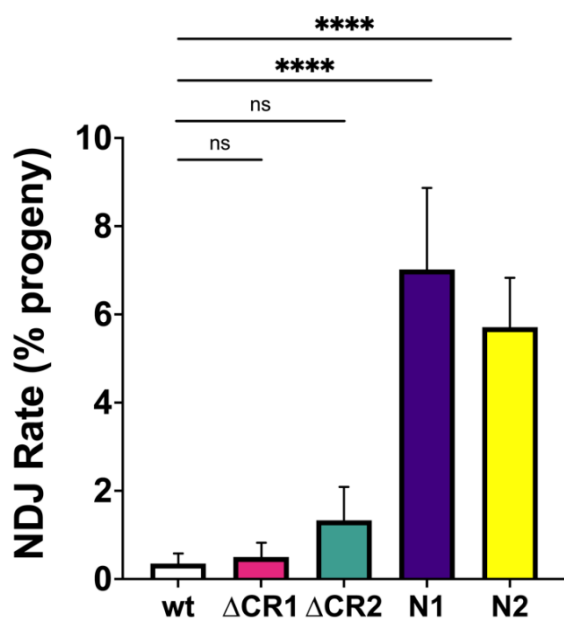


Figure 3. Meiotic non-disjunction (NDJ). Virgin females with the *Blm* alleles indicated on the X-axis over the *Blm*^{N1} null allele (*Blm*^{N1} was over *Blm*^{D2}) were crossed to *y sc cv v g f / Dp(1;Y)B^S* males in at least 15 vials, each serving as a biological replicate. Progeny were scored for non-disjunction (NDJ), indicated by bar eyes in daughters (XXY) and non-bar-eyes in sons (X0) genotypes. The number of NDJ progeny was doubled to correct for genotypes that do not progress to adulthood (XXX and Y0), then NDJ rate was determined as a ratio of the number of corrected NDJ individuals to total progeny for each genotype. Neither *Blm*^{ΔCR1} (ΔCR1) nor *Blm*^{ΔCR2} (ΔCR2) had a significant increase in NDJ compared to wild type (wt). In agreement with prior studied, both *Blm*^{N1} and *Blm*^{N2} females have significantly elevated NDJ. Number of progeny = wt: 6900; ΔCR1: 3593; ΔCR2: 777; N1: 2959; N2: 1906. **** *p* < 0.0001; ns: *p* > 0.05 by the methods described in Zeng *et al.* (4).

121

122 **CR1 and CR2 are required for repair of DSBs by SDSA**

123 *Blm* has a key role in SDSA, where it is thought to promote dissociation of D-loops
124 during or after synthesis (7, 41). To determine whether the lower number of mitotic crossovers in
125 the *Blm*^{ΔCR1} and *Blm*^{ΔCR2} mutants relative to null mutants is due to better capabilities of these
126 alleles to complete SDSA, we conducted the *P*{*w*^a} SDSA assay (7, 41). In this assay,

127 effectiveness of SDSA in the male germline is determined by scoring progeny for a red eye color
 128 that indicates synthesis of >4000 bp from each end of gap generated by transposase-mediated
 129 excision, followed by dissociation of nascent strands and annealing of an internal repeat (the
 130 long terminal repeat of a *copia* retrotransposon). This outcome is greatly reduced in *Blm^{N1}* and
 131 *Blm^{N2}* mutants, demonstrating inability to complete SDSA (3, 7). We found a similar reduction in
 132 *Blm^{ΔCR1}* and *Blm^{ΔCR2}*, (Figure 4), revealing a requirement for both CR1 and CR2 in SDSA repair.
 133

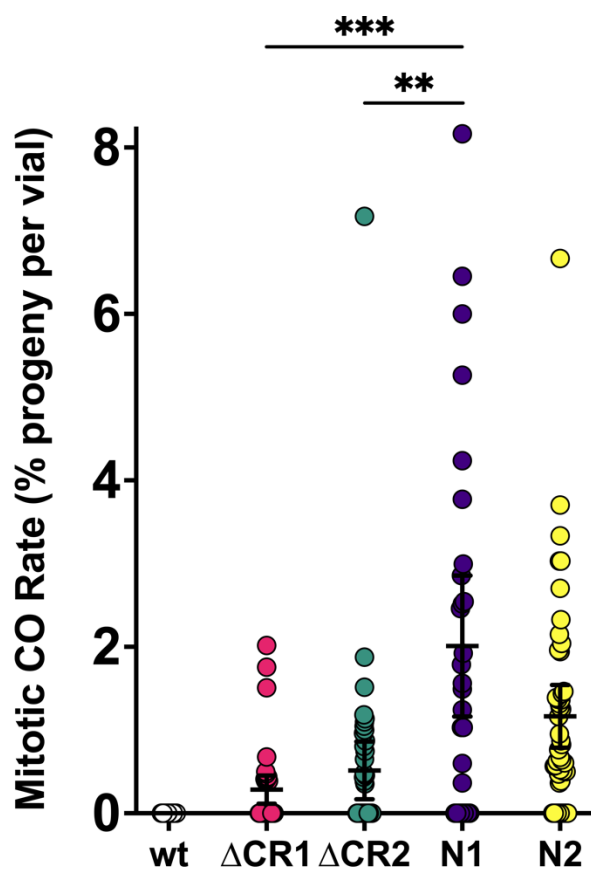


Figure 4. Mitotic crossovers in *Blm* mutants.

Single males with the *Blm* alleles indicated on the X-axis over a the *Blm^{N1}* null allele (or *Blm^{D2}* for *Blm^{N1}*) were crossed to homozygous *net dpp^{ho} dpy b pr cn* recessive phenotypic marker virgin females, with each vials serving as a biological replicate. Progeny were then scored for mitotic crossovers occurring in the parental male's germline, indicated by mixed presence and/or absence of recessive phenotypes. To obtain the mitotic crossover rate per vial, the number of mitotic crossover progeny was divided by the total number of progeny in that vial. Rates for each vial were then pooled to obtain a mean mitotic crossover rate for each genotype. Crossovers are extremely rare in wild-type males (3), so these are excluded from statistical analyses. While both *Blm^{ΔCR1}* (Δ CR1) and *Blm^{ΔCR2}* (Δ CR2) have mitotic crossovers, the rates in both mutants are significantly less than that of the *Blm^{N1}* null mutants (N1). *** $p < 0.001$ and ** $p < 0.01$ by ANOVA with Tukey's Post Hoc. Compared to the separation-of-function *Blm^{N2}*

(N2; $n = 7390$) mutant, Δ CR1 mutants had significantly fewer mitotic crossovers ($p < 0.05$ by ANOVA with Tukey's Post Hoc), but Δ CR2 was not significantly different. $n =$ wt: 37 vials, 7091 progeny; Δ CR1: 54 vials, 9284 progeny; Δ CR2: 44 vials, 7174 progeny; N1: 88 vials, 9368 progeny; N2: 54 vials, 7390 progeny.

134 ***Blm*^{ΔCR1} and *Blm*^{ΔCR2} mutants have distinct meiotic phenotypes compared to *Blm*^{N1} null**
135 **mutants**

136 Loss of Blm causes meiotic non-disjunction (NDJ; Figure 1B) (1, 3). To assess this
137 function in our *Blm* deletion alleles, we performed an X chromosome NDJ assay. The rates of
138 NDJ in *Blm*^{ΔCR1} (0.5%) and *Blm*^{ΔCR2} females (1.33%) were not significantly different from that of
139 wild-type females (Figure 5), indicating that the regions deleted in CR1 and CR2 are
140 dispensable for Blm functions that prevent NDJ. *Blm*^{ΔCR1} and *Blm*^{ΔCR2} each also had significantly
141 lower NDJ rates than *Blm*^{N1} and *Blm*^{N2} females (7.02% and 5.71%, respectively).

142 We also wanted to examine crossing over in *Blm*^{ΔCR1} and *Blm*^{ΔCR2} mutants. Based on
143 results from the NDJ assay, we hypothesized that both *Blm*^{ΔCR1} and *Blm*^{ΔCR2} mutants would
144 have normal meiotic crossovers. Surprisingly, crossovers were significantly reduced in *Blm*^{ΔCR1}
145 mutants (total genetic length of the region assayed was 44.8 cM in *Blm*^{ΔCR1} vs. 52.4 cM in wild-
146 type, $p < 0.0001$), particularly in the middle of the chromosome arm assayed (Figure 6). Also

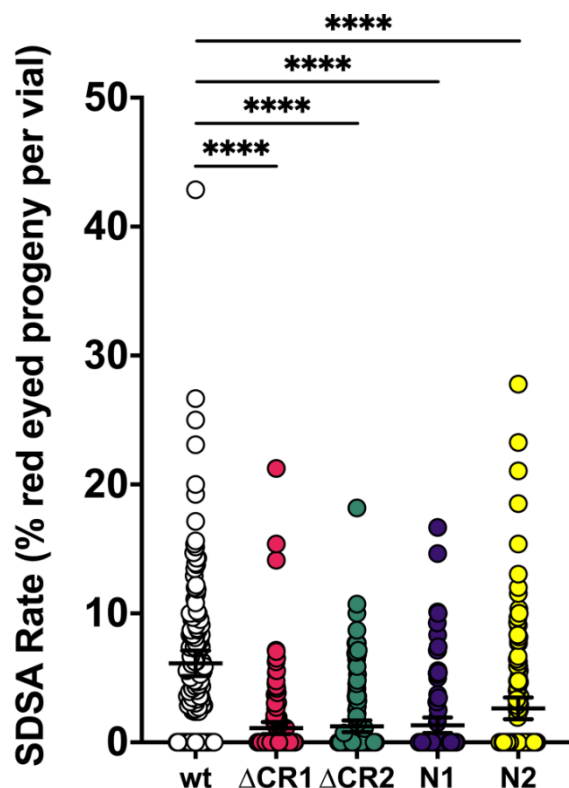


Figure 5. Repair of DNA gaps by SDSA. Single males with the *Blm* alleles indicated on the X-axis (in *trans* to a *Blm*^{D2} null allele) and the Δ2-3 transposase were crossed to homozygous *P{w^a}* virgin females, with each vial serving as a biological replicate. Progeny without the Δ2-3 transposase were scored for the type of repair that occurred in the parental male's germline, with red eyes indicating completed SDSA, yellow or white eyes indicating end-joining, and apricot eyes indicating either no excision or repair that restored the complete *P{w^a}*. SDSA frequency is the percentage of progeny with red eyes. All mutants had significantly lower numbers of red-eyed progeny than wild-type. **** $p < 0.0001$ by ANOVA with Tukey's Post Hoc and Kruskal-Wallis with Dunn's Multiple comparisons. n =wt: 151 vials, 4675 progeny; ΔCR1: 45 vials, 6393 progeny; ΔCR2: 148 vials, 4328 progeny; N1: 106 vials, 4197 progeny; N2: 133 vials, 3860 progeny.

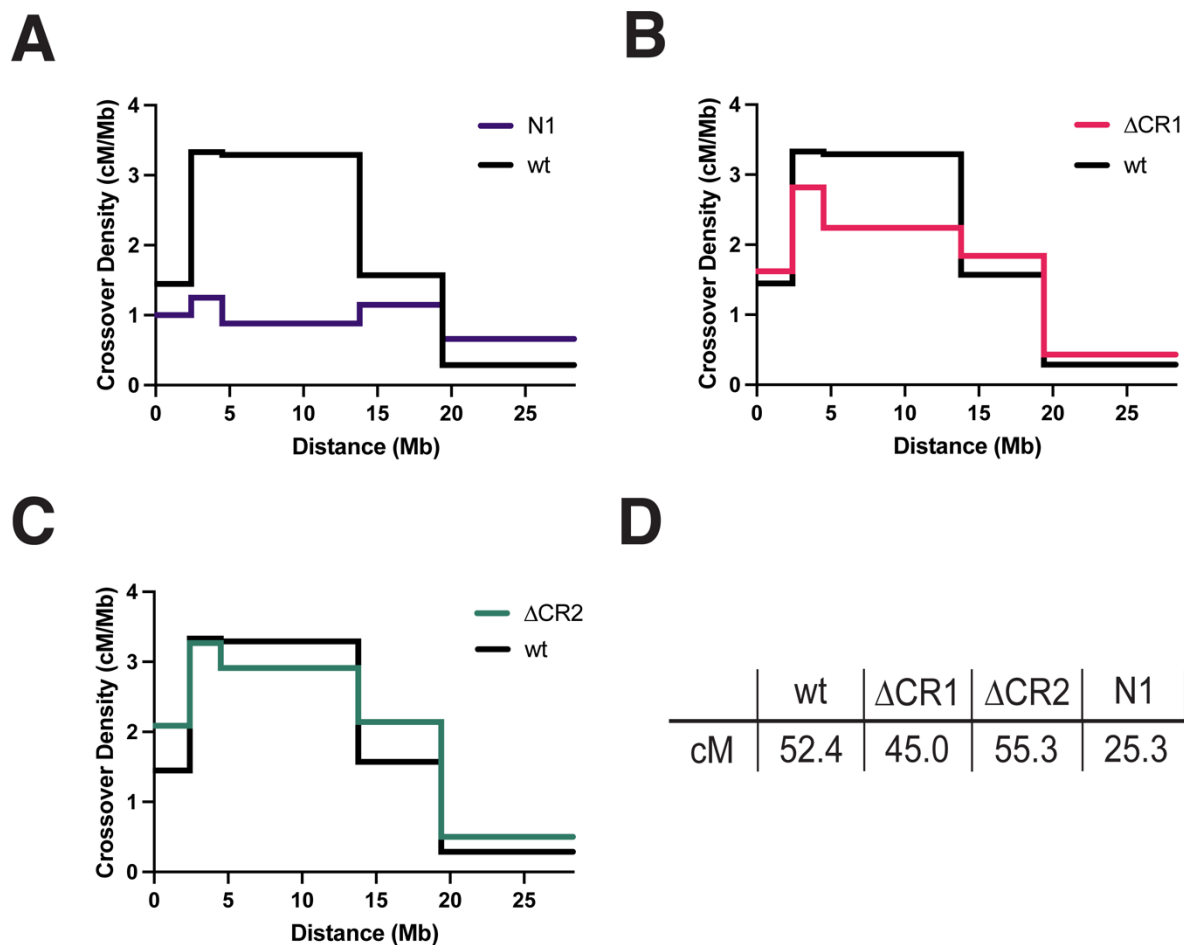


Figure 6. Meiotic Crossovers in *Blm* Mutants. Virgin females with the *Blm* alleles indicated on the X axis (in *trans* so the *Blm*^{N1} null allele or, for *Blm*^{N1}, *Blm*^{D2}) and heterozygous for the *net dpp^{ho} dpy b pr cn* chromosome were test crossed and progeny were scored for recessive phenotypes. Graphs show crossover density (cM/Mb) for each genetic interval. **(A)** *Blm*^{N1} (N1) had a significant reduction in crossovers and an altered distribution, in agreement with a prior study (1). **(B)** Crossovers were significantly reduced in *Blm* ^{Δ CR1} ($p < 0.01$ by Fisher's exact test). **(C)** *Blm* ^{Δ CR2} mutants had a modest but statistically significant increase in crossovers ($p < 0.01$ by Fisher's exact test). **(D)** Both *Blm* ^{Δ CR1} and *Blm* ^{Δ CR2} mutants had significantly higher crossing over than *Blm*^{N1} ($p < 0.0001$ for each, Fisher's exact test for each. $n = 4031$ for wt; 4049 for *Blm* ^{Δ CR1}; 5088 for *Blm* ^{Δ CR2}).

147 surprising was that *Blm* ^{Δ CR2} mutants had significantly more crossovers (55.3 cM vs. 52.4 cM in
 148 wild-type females), with a similar distribution (Figure 6). These results suggest that CR1 and
 149 CR2 have different functions in meiosis, contributing to meiotic crossover distribution in
 150 opposing ways.

151 Discussion

152

153 **CR2 is required for embryonic development**

154 We have shown here that two previously uncharacterized regions of *Drosophila* Blm
155 have distinct functional roles. Embryos from *Blm*^{ΔCR2} homozygous mutant females show
156 compromised hatching, to a similar degree as null mutants. This is likely due to the
157 accumulation of anaphase bridges resulting from defects in rapid replication and/or an inability
158 to resolve sister chromatid entanglements during anaphase. Russell and colleagues (37)
159 mapped a TopII α interaction with human BLM to the region that may correspond to CR2 of
160 *Drosophila* Blm, but this interaction has not been mapped in *Drosophila* Blm. It is possible that
161 this region is regulated to either promote or prevent such interaction. Phosphorylation by ataxia-
162 telangiectasia and *rad3*⁺ related and mutated (ATR/ATM) kinases might be one way to promote
163 interaction with TopII α as part of the DNA damage response, both in stalled fork repair and
164 resolution of anaphase bridges. Human ATR phosphorylates BLM at two residues to promote
165 the recovery of replication forks after stalling by hydroxyurea, and mutation of these residues to
166 alanine results in cell cycle arrest (42). Tangeman and colleagues (43) found that additional
167 predicted ATR/ATM phosphorylation sites are important for BLM nucleolar localization and TopI
168 interaction. The CR2 region has several S/T-Q sites that are possible targets of ATR/ATM
169 phosphorylation, but a *Drosophila* phosphoproteomic analysis did not identify any
170 phosphopeptides from this region in embryos (44).

171 Harris-Behnfeldt and colleagues (45) showed a potential requirement for
172 phosphorylation of the human BLM region analogous to *Drosophila* Blm CR2, identifying several
173 residues that when mutated to alanine increase ultra-fine anaphase bridges and DNA double-
174 strand breaks while decreasing colocalization of BLM and TopII α . While some of these residues
175 were predicted to be phosphorylated by ATR/ATM, others were not, suggesting that regulation

176 may be distinct in different species. Regardless of the kinase, regulation and specifically
177 phosphorylation of this region is important to BLM/Blm interaction with TopII α and function in
178 replication fork repair and resolution of anaphase bridges, even if the residues and kinases
179 involved differ.

180

181 **CR1 and CR2 are required for SDSA and prevention of mitotic crossovers**

182 Both *Blm* ^{Δ CR1} and *Blm* ^{Δ CR2} mutants showed defects in DSB repair. SDSA rates were
183 compromised to the same extent as in *Blm*^{N1} null mutants, but the frequency of spontaneous
184 mitotic crossovers was not as high as in null mutants. One possibility is that CR1 and CR2 are
185 required for SDSA but not for dHJ dissolution. It is not possible to test this possibility *in vivo* due
186 to the lack of a dHJ dissolution assay. CR1 may be analogous to the major TopIII α -interacting
187 region of human BLM (28). *In vitro*, dHJ dissolution requires TopIII α , which might suggest that
188 *Blm* ^{Δ CR1} mutants would be defective for dissolution; however, human TopIII α also interacts with
189 the C-terminus of BLM (28). Interactions between *Drosophila* Blm and TopIII α have not been
190 mapped. Furthermore, although BLM can disassemble short D-loops *in vitro*, it is likely that
191 disassembly of D-loops *in vivo*, where the ends are not free to rotate, requires topoisomerase
192 activity, so loss of this interaction may impair both SDSA and dHJ dissolution.

193 How then might each of the Blm deletions studied lead to compromised SDSA? For
194 CR1, it may be that Blm-TopIII α interaction with both N- and C-terminal regions of Blm together
195 are necessary for effective SDSA, with loss of either leading to disrupted repair. This could be
196 further explored with a C-terminal deletion in examination of SDSA and mitotic crossovers. We
197 attempted to pursue such a mutant, deleting both the final 100 and 150 amino acids in the
198 unstructured C-terminal region of Blm, but both deletions were homozygous lethal, which is
199 unexpected given that *Blm* null mutants are viable. Future studies could also target ATR/ATM

200 predicted phosphorylation residues within CR1 to attempt to characterize the role of regulation
201 of this region in effective SDSA.

202 As for the role of CR2 in SDSA, it may be that an interaction with TopII is required for this
203 process. While TopIII α is likely the primary topoisomerase involved in dissolution of D-loops in
204 SDSA, TopII may be necessary to decatenate more complex DNA structures resulting from
205 errors or disrupted repair. Future directions will also work to characterize the effects of
206 regulation of CR2 on SDSA, with positive regulation potentially promoting additional interaction
207 and/or stabilization.

208

209 **CR1 and CR2 contribute to distinct meiotic processes**

210 The two deletions caused different meiotic phenotypes. *Blm* ^{Δ CR1} mutants had a
211 significant reduction in meiotic COs, whereas *Blm* ^{Δ CR2} mutants had an increase. Neither mutant
212 had increased NDJ. These are both different from *Blm* null mutants, which have decreased
213 meiotic COs, altered CO distribution, and elevated NDJ.

214 CR1 appears to play a role in meiotic CO distribution, but in a way that is not required for
215 proper segregation of meiotic chromosomes. How loss of this region impacts crossovers but not
216 segregation is unknown. While many of the components involved in meiotic and mitotic DNA
217 repair are conserved, their regulation does often differ in each process. CR1 would be
218 hypothesized to be involved in the resolution of meiotic DSBs as COs, but not in their repair as
219 NCOs. This would be explained by a higher incidence of meiotic NCOs in *Blm* ^{Δ CR1} mutants. This
220 might be detectable in whole-genome sequencing of progeny to quantify NCOs. Ability of
221 *Blm* ^{Δ CR1} to resolve any bridged chromosomes during meiotic anaphases could explain the
222 normal NDJ numbers. We should note too that while *Blm* ^{Δ CR1} CO numbers were significantly
223 lower than wild-type, they were much higher than *Blm* null mutants, so the effects on COs may
224 be mild enough to lead to normal meiotic chromosome segregation.

225 Blm^{ΔCR2} meiotic activities are also unusual, with a significant increase of meiotic COs yet
226 normal meiotic disjunction. We speculate that this may be due to an inability of Blm^{ΔCR2} to
227 resolve DSBs as NCOs, sending more of them into a CO pathway. This would be consistent
228 with CR2, but not CR1, being required for meiotic SDSA and/or dHJ dissolution. Consistent with
229 this hypothesis, overall numbers and patterning of crossovers would not be disrupted, possibly
230 due to Blm^{ΔCR2} having an intact CR1.

231

232 **Conclusion**

233 We have assessed genetic functions of N-terminal, unstructured regions of *Drosophila*
234 Blm helicase. We show that deletion of the first 240 amino acids (CR1) does not impair
235 embryonic development or meiotic chromosome segregation but disrupts mitotic DNA repair and
236 meiotic crossover distribution. Deletion of the 146 amino acids upstream of the helicase domain
237 (CR2) leads to severely disrupted embryonic development and aberrant mitotic DNA repair but
238 allows normal meiotic crossover distribution and chromosome segregation. Through this
239 characterization, we have begun to assign distinct Blm functions to different regions of the N-
240 terminus, leading to a better understanding of how this complex protein works to promote
241 development, meiosis, and genome stability.

242

243 **Methods**

244 **CRISPR/Cas9 Deletion of CR1 and CR2**

245 The endogenous CR1 and CR2 region of the *Blm* gene (chromosome 3L, cytological
246 region 86E17) were deleted in-frame using CRISPR/Cas9 genome engineering similar to that
247 described in Lamb *et al.*, 2017 (Figure S2). A plasmid containing DNA homologous to 5' and 3'
248 *Blm* flanking sequence of either CR1 or CR2 (pSL1180 ΔCR1 5'+3' Homology Arms and
249 pSL1180 ΔCR2 5'+3' Homology Arms, respectively) and another plasmid containing 5' and 3'

250 *Blm* gRNAs for CR1 or CR2 were (pCFD4 *Blm* 1+240 gRNA and pCFD4 *Blm* 576+720 gRNA,
251 respectively) were simultaneously injected into *Drosophila* embryos expressing Cas9 in their
252 germline stem cells under control of the *nanos* promoter (Genetivision, Houston, TX). Upon
253 eclosion of these embryos, single male progeny were crossed to *TM3,Sb/TM6B, Hu Tb* females
254 to balance their potentially edited chromosomes. Once balanced, subsequent single male
255 progeny were again mated to *TM3,Sb/TM6B, Hu Tb* females. After being allowed to mate for 3-4
256 days at 25 °C, these single males were collected, frozen, and had their genomic DNA isolated to
257 screen for successful deletions by PCR. For vials in which parental males contained the deletion
258 (indicated by a smaller DNA band after PCR compared to wild-type flies), progeny were then
259 mated to siblings to establish a stock. Each deletion stock was then further screened via
260 genomic extraction, PCR, and sequencing of homozygous flies within the resulting stock to
261 confirm the deletion resulted in the correct sequence and that there were no frameshifts. All
262 homozygotes sequenced from each resulting stock contained the correct deletion, flanking
263 sequence, and were not frameshifted, indicating that CR1 and CR2 were successfully deleted.

264

265 **Embryonic Hatching Assay**

266 20-30 virgin females homozygous for each *Blm* allele were crossed to 15 *Oregon-RM*
267 (wild-type) males and allowed to acclimate to grape-juice agar plates with yeast paste for 24-36
268 hrs at 25 °C. Plates were then changed and embryos were collected overnight (16 hrs) at 25 °C.
269 150-300 embryos were then transferred to a gridded grape juice agar plate (10/grid) and scored
270 for hatching after 48 hours at 25 °C. Hatch assays were completed in three replicates for each
271 allelic condition, with a minimum of 550 total embryos assayed per condition.

272

273 **Meiotic Non-disjunction Assay**

274 Female meiotic non-disjunction (NDJ) of the X chromosome was measured by first
275 crossing *w; Blm^{N1}/TM3, Sb* virgin females to *Oregon-RM* (wild-type) males or males with the

276 *Blm* allele of interest (*Blm*^{N2}, *Blm*^{ΔCR1}, or *Blm*^{ΔCR2}) balanced over either *TM3*, *Sb* or *TM6B*, *Hu Tb*
277 to generate heteroallelic *Blm* females (e.g., *Blm*^{N1} / *Blm*^{N2}). For experiments with *Blm*^{N1} only,
278 *Blm*^{N1} *ry e P{UASp::Blm}* / *TM6B*, *Hu Tb* virgin females were crossed *meiP22*¹⁰³ *st Blm*^{D2} *ry rec*¹
279 *Ubx P{matα::GAL4}* / *TM6B*, *Hu Tb* males to generate heteroallelic *Blm* null females that could
280 rescue *Blm* expression after meiotic chromosome segregation to prevent maternal-effect
281 lethality. *Blm*^{D2} is another null allele of *Blm* that contains a premature stop codon in the helicase
282 domain (Kusano, 2001). Heteroallelic *Blm* females were then crossed to *y sc cv v g f /*
283 *Dp(1;Y)B^S* males. The duplication on the Y chromosome carries a dominant mutation causing
284 bar-shaped eyes. Normal progeny resulting from this cross are females whose eyes are *Bar*⁺
285 and males whose eyes are *Bar*. Non-disjoined ova that are diplo-X result in *XXY* females (and
286 *XXX* progeny who do not survive) whose eyes are *Bar*. Non-disjoined ova that are nullo-X result
287 in *X0* males (and *Y0* progeny who do not survive) whose eyes are *Bar*⁺. *X NDJ* is calculated as
288 the percentage of progeny that arose from NDJ (*Bar* females and *Bar*⁺ males), correcting for
289 the loss of half of the diplo- and nullo-X ova by multiplying this percentage by two. Crosses were
290 set up as ten females and four males/vial for *Oregon-RM* (wild-type), *Blm*^{ΔCR1}, and *Blm*^{N2}
291 genotypes and thirty females and eight males for *Blm*^{ΔCR2} and *Blm*^{N1} genotypes. Data were
292 pooled from between 15-60 vials and at least 1000 total progeny to determine the mean NDJ
293 rate for each genotype.

294

295 **Mitotic Crossover Assay**

296 Pre-meiotic mitotic crossovers were measured in the male germline using the *net dpp*^{ho}
297 *dpy b pr cn* recessive phenotypic marker chromosome. Virgin females with *net dpp*^{ho} *dpy b pr*
298 *cn/ SM6a* and wild-type or various *Blm* alleles (*Blm*^{N2}, *Blm*^{ΔCR1}, or *Blm*^{ΔCR2}) balanced over *TM6B*,
299 *Hu Tb* were crossed to *w; Blm*^{N1} / *TM3*, *Sb* to generate single males heteroallelic (e.g. *Blm*^{N2} /
300 *Blm*^{N1}) for *Blm* and heterozygous for recessive phenotypic markers for mitotic crossover
301 analysis. For *Blm*^{N1} only, virgin females were instead crossed to *w; Blm*^{D2} / *TM3*, *Sb*. Single

302 males for each genotype were then crossed to homozygous *net dpp^{ho} dpy b pr cn* females and
303 scored for mitotic crossovers indicated by the mixed presence and/or absence of recessive
304 phenotypic markers in progeny. Progeny for each single male was scored as a ratio of
305 crossover progeny to total progeny to generate a mitotic crossover rate for each vial. Data for
306 each genotype were pooled from at least 38 vials and 7000 progeny to determine the mean
307 mitotic crossover rate.

308

309 **P{w^a} Assay**

310 The P{w^a} was performed as described previously (Adams et al., 2003), with minor
311 modifications. First, y² w^Δ P{w^a} virgin females with wild-type or various *Blm* alleles (*Blm^{N1}*,
312 *Blm^{N2}*, *Blm^{ΔCR1}*, or *Blm^{ΔCR2}*) balanced over *TM6B, Hu Tb* were crossed to *st P{Δ2-3} Blm^{D2} Sb/
313 TM6B, Hu Tb* males to generate single males that were heteroallelic for *Blm* (e.g. *Blm^{N1} / Blm^{D2}*)
314 with the P{w^a} insertion and the Δ2-3 transposase. Single males for each genotype were then
315 crossed to y² w^Δ P{w^a} and progeny were scored for efficiency of repair by resulting eye color:
316 red indicating efficient SDSA, white/yellow indicating end-joining, and apricot indicating no
317 cutting or perfect repair. Progeny from each single male was scored as a ratio of red-eyed
318 progeny to total progeny as a measure of SDSA repair rate. Data for each genotype were
319 pooled from at least 160 vials and 3800 progeny to determine the mean SDSA repair rate.

320

321 **Meiotic Crossover Assay**

322 Meiotic crossovers were measured in the female germline using the *net dpp^{ho} dpy b pr*
323 *cn* recessive phenotypic marker chromosome. Virgin females with *net dpp^{ho} dpy b pr cn / SM6a*
324 and wild-type or various *Blm* alleles (*Blm^{ΔCR1}* or *Blm^{ΔCR2}*) combined with P{matα::GAL4} for
325 maternal-effect lethality rescue were crossed to *Blm^{N1} ro e P{UASp::Blm} / TM6B, Hu Tb* to
326 generate females heteroallelic for *Blm* and heterozygous for recessive phenotypic markers for
327 meiotic crossover analysis. For *Blm^{N1}* only, *net dpp^{ho} dpy b pr cn / CyO; Blm^{N1} r e P{UASp::Blm}*

328 *TM6B, Hu Tb* virgin females were instead crossed to *mei-P22¹⁰³ st Blm^{D2} ry rec¹ Ubx*
329 *P{mataα::GAL4} / TM6B, Hu Tb*. Virgin females for each genotype were then crossed to
330 homozygous *net dpp^{ho} dpy b pr cn* males and scored for meiotic crossovers indicated by the
331 mixed presence and/or absence of recessive phenotypic markers in progeny. Progeny was
332 scored as a ratio of crossover progeny to total progeny to generate a meiotic crossover rate.
333 Data for each genotype were pooled from at least 38 vials and 7000 progeny to determine the
334 mean mitotic crossover rate.

335

336 Acknowledgements

337 We thank members of the Sekelsky lab for helpful comments on the manuscript. This work was
338 supported by a grant from the National Institute of General Medical Sciences to JS under award
339 1R35GM118127. EBD was supported in part by a grants from the National Cancer Institute (T32
340 CA217824). The funders did not play any role in study design, data collection and analysis,
341 decision to publish, or preparation of the manuscript.

342

343 The authors declare that they have no competing interests.

344

345 References

- 346 1. Hatkevich T, Kohl KP, McMahan S, Hartmann MA, Williams AM, Sekelsky J. Bloom syndrome
347 helicase promotes meiotic crossover patterning and homolog disjunction. *Curr Biol.*
348 2017;27(1):96-102.
- 349 2. Cheok CF, Wu L, Garcia PL, Janscak P, Hickson ID. The Bloom's syndrome helicase promotes
350 the annealing of complementary single-stranded DNA. *Nucleic Acids Res.* 2005;33(12):3932-
351 41.
- 352 3. McVey M, Andersen SL, Broze Y, Sekelsky J. Multiple functions of *Drosophila* BLM helicase in
353 maintenance of genome stability. *Genetics.* 2007;176(4):1979-92.
- 354 4. Zeng Y, Li H, Schweppe NM, Hawley RS, Gilliland WD. Statistical analysis of nondisjunction
355 assays in *Drosophila*. *Genetics.* 2010;186(2):505-13.
- 356 5. Ellis NA, Groden J, Ye TZ, Straughen J, Lennon DJ, Ciocci S, et al. The Bloom's syndrome
357 gene product is homologous to RecQ helicases. *Cell.* 1995;83(4):655-66.
- 358 6. Larsen NB, Hickson ID. RecQ helicases: Conserved guardians of genomic integrity. *Adv Exp*
359 *Med Biol.* 2013;767:161-84.

- 360 7. Adams MD, McVey M, Sekelsky J. *Drosophila* BLM in double-strand break repair by synthesis-
361 dependent strand annealing. *Science*. 2003;299(5604):265-7.
- 362 8. Dutertre S, Ababou M, Onclercq R, Delic J, Chatton B, Jaulin C, et al. Cell cycle regulation of
363 the endogenous wild type Bloom's syndrome DNA helicase. *Oncogene*. 2000;19(23):2731-8.
- 364 9. Imamura O, Fujita K, Shimamoto A, Tanabe H, Takeda S, Furuichi Y, et al. Bloom helicase is
365 involved in DNA surveillance in early S phase in vertebrate cells. *Oncogene*.
366 2001;20(10):1143-51.
- 367 10. Brady MM, McMahan S, Sekelsky J. Loss of *Drosophila* Mei-41/ATR alters meiotic crossover
368 patterning. *Genetics*. 2018;208(2):579-88.
- 369 11. LaFave MC, Andersen SL, Stoffregen EP, Korda Holsclaw J, Kohl KP, Overton LJ, et al.
370 Sources and structures of mitotic crossovers that arise when BLM helicase is absent in
371 *Drosophila*. *Genetics*. 2014;196(1):107-18.
- 372 12. Wu L. Role of the BLM helicase in replication fork management. *DNA Repair (Amst)*.
373 2007;6(7):936-44.
- 374 13. Wu L, Hickson ID. The Bloom's syndrome helicase suppresses crossing over during
375 homologous recombination. *Nature*. 2003;426(6968):870-4.
- 376 14. Hatkevich T, Sekelsky J. Bloom syndrome helicase in meiosis: Pro-crossover functions of an
377 anti-crossover protein. *Bioessays*. 2017;39(9).
- 378 15. Cox RL, Hofley CM, Tatapudy P, Patel RK, Dayani Y, Betcher M, et al. Functional conservation
379 of RecQ helicase BLM between humans and *Drosophila melanogaster*. *Scientific reports*.
380 2019;9(1):17527.
- 381 16. Ruchert JM, Brady MM, McMahan S, Lacey KJ, Latta LC, Sekelsky J, et al. Blm helicase
382 facilitates rapid replication of repetitive DNA sequences in early *Drosophila* development.
383 *Genetics*. 2022;220(1).
- 384 17. Ababou M. Bloom syndrome and the underlying causes of genetic instability. *Molecular*
385 *genetics and metabolism*. 2021;133(1):35-48.
- 386 18. Payne M, Hickson ID. Genomic instability and cancer: lessons from analysis of Bloom's
387 syndrome. *Biochem Soc Trans*. 2009;37(Pt 3):553-9.
- 388 19. Luo G, Santoro IM, McDaniel LD, Nishijima I, Mills M, Youssoufian H, et al. Cancer
389 predisposition caused by elevated mitotic recombination in Bloom mice. *Nat Genet*.
390 2000;26(4):424-9.
- 391 20. Goss KH, Risinger MA, Kordich JJ, Sanz MM, Straughen JE, Slovek LE, et al. Enhanced
392 tumor formation in mice heterozygous for *Blm* mutation. *Science*. 2002;297(5589):2051-3.
- 393 21. Gruber SB, Ellis NA, Scott KK, Almog R, Kolachana P, Bonner JD, et al. BLM heterozygosity
394 and the risk of colorectal cancer. *Science*. 2002;297(5589):2013.
- 395 22. Lindor NM, Larson MC, DeRycke MS, McDonnell SK, Baheti S, Fogarty ZC, et al. Germline
396 miRNA DNA variants and the risk of colorectal cancer by subtype. *Genes Chromosomes*
397 *Cancer*. 2017;56(3):177-84.
- 398 23. Chaganti RS, Schonberg S, German J. A manyfold increase in sister chromatid exchanges in
399 Bloom's syndrome lymphocytes. *Proc Natl Acad Sci USA*. 1974;71(11):4508-12.
- 400 24. German J, Schonberg S, Louie E, Chaganti RS. Bloom's syndrome. IV. Sister-chromatid
401 exchanges in lymphocytes. *Am J Hum Genet*. 1977;29(3):248-55.
- 402 25. Bachrati CZ, Borts RH, Hickson ID. Mobile D-loops are a preferred substrate for the Bloom's
403 syndrome helicase. *Nucleic Acids Res*. 2006;34(8):2269-79.

- 404 26. Karow JK, Constantinou A, Li JL, West SC, Hickson ID. The Bloom's syndrome gene product
405 promotes branch migration of holliday junctions. *Proc Natl Acad Sci USA*. 2000;97(12):6504-8.
- 406 27. van Brabant AJ, Ye T, Sanz M, German IJ, Ellis NA, Holloman WK. Binding and melting of D-
407 loops by the Bloom syndrome helicase. *Biochemistry*. 2000;39(47):14617-25.
- 408 28. Wu L, Davies S, North P, Goulaouic H, Riou J, Turley H, et al. The Bloom's syndrome gene
409 product interacts with topoisomerase III. *J Biol Chem*. 2000;275(13):9636 - 44.
- 410 29. Sekelsky J. DNA repair in *Drosophila*: Mutagens, models, and missing genes. *Genetics*.
411 2017;205(2):471-90.
- 412 30. Plank JL, Wu J, Hsieh TS. Topoisomerase III α and Bloom's helicase can resolve a mobile
413 double Holliday junction substrate through convergent branch migration. *Proc Natl Acad Sci*
414 *USA*. 2006;103(30):11118-23.
- 415 31. Raynard S, Bussen W, Sung P. A double Holliday junction dissolvasome comprising BLM,
416 topoisomerase III α , and BLAP75. *J Biol Chem*. 2006;281(20):13861-4.
- 417 32. Wu L, Chan KL, Ralf C, Bernstein DA, Garcia PL, Bohr VA, et al. The HRDC domain of BLM is
418 required for the dissolution of double Holliday junctions. *EMBO J*. 2005;24(14):2679-87.
- 419 33. Ralf C, Hickson ID, Wu L. The Bloom's syndrome helicase can promote the regression of a
420 model replication fork. *J Biol Chem*. 2006.
- 421 34. Davies SL, North PS, Hickson ID. Role for BLM in replication-fork restart and suppression of
422 origin firing after replicative stress. *Nat Struct Mol Biol*. 2007;14(7):677-9.
- 423 35. Chan KL, North PS, Hickson ID. BLM is required for faithful chromosome segregation and its
424 localization defines a class of ultrafine anaphase bridges. *EMBO J*. 2007;26(14):3397-409.
- 425 36. Seki M, Nakagawa T, Seki T, Kato G, Tada S, Takahashi Y, et al. Bloom helicase and DNA
426 topoisomerase III α are involved in the dissolution of sister chromatids. *Mol Cell Biol*.
427 2006;26(16):6299-307.
- 428 37. Russell B, Bhattacharyya S, Keirse J, Sandy A, Grierson P, Perchiniak E, et al. Chromosome
429 breakage is regulated by the interaction of the BLM helicase and topoisomerase II α .
430 *Cancer Res*. 2011;71(2):561-71.
- 431 38. Mann MB, Hodges CA, Barnes E, Vogel H, Hassold TJ, Luo G. Defective sister-chromatid
432 cohesion, aneuploidy and cancer predisposition in a mouse model of type II Rothmund-
433 Thomson syndrome. *Hum Mol Genet*. 2005;14(6):813-25.
- 434 39. Naim V, Rosselli F. The FANC pathway and BLM collaborate during mitosis to prevent micro-
435 nucleation and chromosome abnormalities. *Nat Cell Biol*. 2009;11(6):761-8.
- 436 40. Grierson PM, Acharya S, Groden J. Collaborating functions of BLM and DNA topoisomerase I
437 in regulating human rDNA transcription. *Mutat Res*. 2013;743-744:89-96.
- 438 41. McVey M, Larocque JR, Adams MD, Sekelsky JJ. Formation of deletions during double-strand
439 break repair in *Drosophila* DmBlm mutants occurs after strand invasion. *Proc Natl Acad Sci*
440 *USA*. 2004;101(44):15694-9.
- 441 42. Davies SL, North PS, Dart A, Lakin ND, Hickson ID. Phosphorylation of the Bloom's syndrome
442 helicase and its role in recovery from S-phase arrest. *Mol Cell Biol*. 2004;24(3):1279-91.
- 443 43. Tangeman L, McIlhatton MA, Grierson P, Groden J, Acharya S. Regulation of BLM nucleolar
444 localization. *Genes*. 2016;7(9).
- 445 44. Zhai B, Villen J, Beausoleil SA, Mintseris J, Gygi SP. Phosphoproteome analysis of *Drosophila*
446 *melanogaster* embryos. *Journal of proteome research*. 2008;7(4):1675-82.

Blm Helicase IDR Functions

Bereda and Dewey *et al.*

- 447 45. Behnfeldt JH, Acharya S, Tangeman L, Gocha AS, Keirse J, Groden J. A tri-serine cluster
448 within the topoisomerase IIalpha-interaction domain of the BLM helicase is required for
449 regulating chromosome breakage in human cells. *Hum Mol Genet.* 2018;27(7):1241-51.
450